

Metallicity measurements using atomic lines in M and K dwarf stars

Vincent M. Woolf^{1*} and George Wallerstein^{1*} †

¹*Astronomy Department, University of Washington, Box 351580, Seattle, WA 98195, USA*

ABSTRACT

We report the first survey of chemical abundances in M and K dwarf stars using atomic absorption lines in high resolution spectra. We have measured Fe and Ti abundances in 35 M and K dwarf stars using equivalent widths measured from $\lambda/\Delta\lambda \approx 33\,000$ spectra. Our analysis takes advantage of recent improvements in model atmospheres of low-temperature dwarf stars. The stars have temperatures between 3300 and 4700 K, with most cooler than 4100 K. They cover an iron abundance range of $-2.44 < [\text{Fe}/\text{H}] < +0.16$. Our measurements show $[\text{Ti}/\text{Fe}]$ decreasing with increasing $[\text{Fe}/\text{H}]$, a trend similar to that measured for warmer stars where abundance analysis techniques have been tested more thoroughly. This study is a step toward the observational calibration of procedures to estimate the metallicity of low-mass dwarf stars using photometric and low-resolution spectral indices.

Key words: stars: abundances – stars: late-type – stars: subdwarfs.

1 INTRODUCTION

Low mass (M dwarf and cooler) main sequence stars are by far the most numerous stars in the Galaxy and make up most of its baryonic mass. However, there have been few detailed chemical abundance studies of these stars with spectra of sufficient resolution for atomic absorption lines to be measured individually. None of these included more than a few stars. This was largely a result of their low intrinsic luminosity and the molecular lines present in their spectra. Their faintness meant that few of these stars were bright enough for high signal to noise, high resolution spectra to be measured easily without a large telescope. The molecular bands present in their spectra complicated the calculation of stellar model atmospheres and cause line blends which make it difficult to measure atomic line strengths in large regions of the visible spectrum. There have been abundance studies which used photometry or which fitted broad molecular features in low-resolution spectra of M and K dwarfs, but their results are not as certain as they would be if they were calibrated

with stars for which more precise abundances were based on higher-resolution spectra. There have also been studies which used synthetic spectrum fitting of low resolution spectra to measure metallicities of low mass dwarfs. These have given rough metallicity estimates, but have not produced elemental abundances with the precision which is possible using higher resolution spectra.

Recent advances in model atmospheres of low mass dwarf stars, largely as a result of the improved treatment of molecular opacity, have provided the opportunity to determine abundances of M and K dwarf stars through analysis of their atomic spectral lines. Our study of chemical abundances in Kapteyn’s Star (HD 33793) (Woolf & Wallerstein 2004) showed us that it is possible to locate spectral regions in these stars where molecular bands are not present or are sufficiently weak for accurate equivalent widths of atomic lines to be measured.

The survey of abundance estimates we report here will provide some of the data necessary to calibrate metallicity indices for cool dwarf stars, for example the TiO and CaH indices of Reid, Hawley, & Gizis (1995) and Hawley, Gizis, & Reid (1996). With calibrated indices it should be possible to estimate the metallicity of a much larger number of cool dwarfs, including those too distant and faint to study using high resolution spectra. When a large volume-limited sample is available, it will be possible to determine if the ‘G dwarf problem’ (van den Bergh 1962; Audouze & Tinsley 1976) continues to lower-mass main sequence stars so that low-metallicity M dwarfs are more scarce than expected in our Galaxy.

* E-mail: vmw@astro.washington.edu (VMW); wall@astro.washington.edu (GW)

† Based on observations obtained with the Apache Point Observatory 3.5-meter telescope, which is owned and operated by the Astrophysical Research Consortium. This publication makes use of data products from the Two Micron All Sky Survey, which is a joint project of the University of Massachusetts and the Infrared Processing and Analysis Center/California Institute of Technology, funded by the National Aeronautics and Space Administration and the National Science Foundation.

2 OBSERVATIONS AND REDUCTION

We selected stars for observation to cover a large range of metallicity: low metallicity stars are overrepresented in our sample compared to the actual number in the solar neighborhood. We increased the number of low metallicity stars by choosing to observe stars with high radial velocities, which increased the likelihood of observing halo stars, and by observing stars with TiO indices (Gizis 1997) which indicate weak TiO band strengths.

Our spectrum of Kapteyn’s Star was measured with the echelle spectrograph of the 4.0-m Victor M. Blanco Telescope at the Cerro Tololo Inter-American Observatory as described in Woolf & Wallerstein (2004). The 34 other stars were observed using the echelle spectrograph of the Apache Point Observatory (APO) 3.5-meter telescope.

The spectra were reduced using standard IRAF routines to subtract the bias, divide by flat field spectra, reduce the echelle orders to one dimensional spectra, and apply ThAr lamp spectrum wavelength calibration. The spectrum of a hot, high $v \sin i$ star was used to correct for telluric absorption lines where appropriate and possible.

The spectral resolution of the APO spectra is about $\lambda/\Delta\lambda \approx 33\,000$, as measured using the ThAr comparison lines. There are no gaps in wavelength between echelle orders. The usable spectrum covers the range from about 9800 Å to where the measured signal from these red stars drops off in the blue, normally below 5000 Å. For most stars, the signal to noise ratio in the region of the lines we used for the analysis was at least 100 per pixel. It was much higher for the brighter stars ($V \lesssim 11$) in our sample. For the faintest star, LHS 364, we were only able to achieve a signal to noise ratio of about 50 with the observation time available.

3 ANALYSIS

3.1 Stellar parameters and model

As we found in our analysis of Kapteyn’s Star, the chemical abundances we derive for these low-temperature dwarf stars depends strongly on the metallicity of the model atmosphere used. For example, changing the metallicity of the model atmosphere with $T_{\text{eff}} = 3500$ K and $\log g = 5.0$ by ± 0.5 dex can change the Fe abundance derived using the equivalent widths measured for Kapteyn’s Star by ± 0.3 dex. Determining the physical parameters to use for the model atmospheres is therefore an iterative process. Fortunately, the iteration converges so it is possible to find the value where the metallicity derived equals the metallicity of the model atmosphere used in the analysis.

We integrated the flux in the V , H , and K_S filters for a grid of synthetic spectra released with the NextGen models (Hauschildt, Allard, & Baron 1999) to produce theoretical colour-temperature relation estimates. We obtained H and K_S magnitudes from the 2MASS point source catalog (Cutri et al. 2003) and V from Mermilliod, Mermilliod, & Hauck (1997) and used these to find $V - K_S$ and $V - H$ temperatures for our stars. We used the average of the two as T_{eff} in our models. We note that while there are few other published determinations of temperatures in the stars we observed, we were happy to see that the temperature we derive for HD 88230, $T_{\text{eff}} =$

3970 ± 220 K, is in good agreement with the temperature derived by Ramírez & Meléndez (2004), $T_{\text{eff}} = 3962 \pm 63$ K, using its bolometric flux and its measured angular diameter.

For stars where parallax data was available we calculated absolute H and K_S magnitudes. We used these to estimate the masses using the theoretical mass-luminosity relations plotted by Ségransan et al. (2003a). We calculated the bolometric correction BC_K from the BC_V and $V - K$ NextGen colours (Hauschildt et al. 1999) and used parallax, K_S and BC_K to derive M_{bol} . We then used M_{bol} , mass, and T_{eff} to calculate $\log g$:

$$\log g = \log M + 4 \log(T_{\text{eff}}/5770) + 0.4(M_{\text{bol}} - 4.65) + 4.44$$

where we have used $T_{\text{eff}\odot} = 5770$ K, $M_{\text{bol}\odot} = 4.65$, $\log g_{\odot} = 4.44$, and M is in solar masses. For stars where parallax measurements were unavailable we assumed $\log g = 5.0 \pm 0.5$. Gravity does not have an effect on the derived chemical abundances as large as the effects of temperature or model metallicity: accepting this large gravity uncertainty does not produce a large uncertainty in the abundances. The parallaxes and magnitudes used to derive the stellar physical parameters are listed in Table 1. Spectral types are included in the table to give a rough idea of how low resolution spectra of the stars appear: the temperatures and gravities derived for the stars and reported in Table 2 are more physically meaningful.

We obtained from P. Hauschildt (private communication) an updated NextGen model atmosphere grid which improves on the most recent public release (Hauschildt et al. 1999) by including the improved TiO and H₂O line lists described in Allard et al. (2000) in its calculation. We used this to create model atmospheres interpolated in $\log g$ and T_{eff} for each star.

For each star we began by assuming a metallicity of $[M/H] = -1.0$.¹ The calculated Fe and Ti abundances were used to estimate the model atmosphere metallicity to be used in the next iteration. The temperature and gravity calculated for the stars also depend on the assumed metallicity, so these also varied during the iteration process. This procedure was repeated until the metallicity derived from the abundances equalled that of the model atmosphere used to calculate them. We note that in this case we define the “metallicity” value by the effect of metals in the stellar atmosphere, primarily through their effect on continuous opacity, not by the total concentration of all elements heavier than He.

Model metallicity corrections due to non-solar $[\alpha/\text{Fe}]$ abundances were estimated using the LTE stellar analysis program MOOG (Snedden 1973) output. The average Ti abundance at a star’s $[\text{Fe}/\text{H}]$ was used as a proxy for the star’s α element enhancement. MOOG provides partial pressures of requested species at the different layers of the model atmosphere, so by finding, for example, the Mg I and Mg II partial pressures we were able to estimate the fraction of Mg which is ionized at the model layer where the reference opacity (at 1.2 μm) is about 0.1, approximately where the lines in which we are interested are formed. The ionization fractions of Na, Mg, Ca, Al, and Fe, the major electron donors, were found for each model in the grid, and thus the fraction

¹ We use the standard notation $[X] \equiv \log_{10}(X)_{\text{star}} - \log_{10}(X)_{\odot}$.

Table 1. M and K dwarf magnitudes and parallaxes

Star	Alternate name	Spectral type ^b	V	±	K _s	±	H	±	π mas	± mas	π source ^a
HD 33793	GJ 191	sdM1.0	8.85	0.03	5.05	0.02	5.32	0.03	255.1	0.9	H
HD 36395	GJ 205	M1.5	7.96	0.01	4.04	0.26	4.15	0.21	175.7	1.2	H
HD 88230	GJ 380	K5	6.60	0.02	2.96	0.29	3.30	0.26	205.2	0.8	H
HD 95735	GJ 411	M2V	7.49	0.02	3.25	0.31	3.64	0.20	392.5	0.9	H
HD 97101B	GJ 414B	M1.5	9.98	0.04	5.73	0.02	5.98	0.02	83.8	1.1	H
HD 119850	GJ 526	M1.5	8.46	0.01	4.42	0.02	4.78	0.21	184.1	1.3	H
HD 178126	G 22-15	K5V	9.23	0.02	6.47	0.02	6.57	0.02	41.2	1.3	H
HD 199305	GJ 809	M0.5	8.54	0.04	4.62	0.02	4.92	0.06	142.0	0.8	H
HD 217987	GJ 887	M0.5	7.35	0.02	3.46	0.20	3.61	0.23	303.9	0.9	H
LHS 12	HIP 9560	M0.5	12.26	0.04	8.68	0.02	8.90	0.03	36.1	4.3	H
LHS 38	GJ 412A	M0.5	8.75	0.04	4.77	0.02	5.00	0.02	206.9	1.2	H
LHS 42	GJ 9371	sdM0.0	12.20	0.03	8.67	0.02	8.90	0.02	44.3	2.8	H
LHS 104	G 30-48	esdK7	13.74	0.02	10.41	0.02	10.57	0.03	19.3	3.0	Y
LHS 170	HIP 15234	sdK	10.68	0.01	7.60	0.02	7.77	0.03	30.2	2.4	H
LHS 173	HIP 16209	sdK7	11.11	0.01	7.79	0.02	7.97	0.02	39.2	2.5	H
LHS 174	G 38-2	sdM0.5	12.75	0.01	9.14	0.02	9.35	0.02	22.6	7.4	Y
LHS 182	GJ 1064D	esdM0.0	13.90	0.02	10.52	0.02	10.67	0.03	23.1	2.8	Y
LHS 236	G 251-44	sdK7	13.10	0.01	9.85	0.02	10.00	0.02	18.2	2.9	Y
LHS 343	G 61-21	sdK	13.82	0.02	10.66	0.02	10.86	0.02	18.6	3.7	Y
LHS 364	GJ 3825	esdM1.5	14.55	0.03	10.86	0.01	11.01	0.02	36.1	3.2	Y,N
LHS 450	GJ 687	M3	9.15	0.03	4.55	0.02	4.77	0.03	220.9	0.9	H
LHS 467	HIP 91668	esdK7	12.21	0.03	8.78	0.02	9.00	0.02	26.0	3.6	H
LHS 1138	G 60-18	G - K	13.29	0.01	10.76	0.02	10.92	0.02	9.5	4.6	Y
LHS 1482	L 586-41	K	13.96	0.03	10.82	0.02	10.98	0.02			
LHS 1819	HIP 28940	K4	10.88	0.02	8.29	0.03	8.37	0.05	17.0	2.6	H
LHS 1841	L 812-11	K	13.18	0.03	10.39	0.02	10.51	0.02	17.5	3.3	Y
LHS 2161	G 48-21	K5	11.58	0.01	8.75	0.02	8.83	0.05			
LHS 2463	G 10-53	K7	12.48	0.01	9.83	0.02	9.99	0.03			
LHS 2715	GJ 506.1	sdK	10.84	0.02	8.17	0.02	8.31	0.03	27.9	2.5	H
LHS 2938	HIP 71122	K7	10.67	0.02	7.76	0.02	7.95	0.05	19.0	2.0	H
LHS 3084	G 15-26	sdK	13.43	0.03	9.78	0.02	9.99	0.03	19.1	2.9	Y
LHS 3356	GJ 701	M1	9.37	0.03	5.31	0.02	5.57	0.04	128.3	1.4	H
LHS 5337	G 21-12	M0	11.15	0.03	7.47	0.02	7.66	0.05	34.5	3.3	H
G 39-36	G 86-10		12.36	0.01	9.54	0.02	9.76	0.03			
HIP 27928	GJ 9192	K4	10.70	0.02	7.76	0.02	7.88	0.03	26.1	2.1	H

^a H: ESA (1997), Y: van Altena, Lee, & Hoffleit (1995), N: Harrington & Dahn (1980), we assume that HD 97101B has the same parallax as HD 97101A

^b taken from Gizis (1997), SIMBAD, Lee (1984), and Luyten (1979)

of free electrons provided by the α elements Mg and Ca were estimated. The model metallicity then used for a star was adjusted to account for how the free electron density was affected by the non-solar $[\alpha/\text{Fe}]$ abundances. The majority of the continuous opacity in the line-forming regions in the atmospheres of these cool dwarfs is provided by the H^- ion, and is thus proportional to the number of free electrons.

For Kapteyn's Star (HD 33793) we used the temperature and gravity derived by Ségransan et al. (2003b) using radius measurements the Very Large Telescope Interferometer, rather than using our photometry and parallax procedure.

The microturbulence parameter was estimated by requiring that there be no slope in Ti abundance vs equivalent width. At the temperatures of these stars, Ti lines are more common than the Fe lines which are normally used for this purpose in warmer stars.

3.2 Chemical abundances

For this survey we have chosen to report our results only for Fe and Ti since there are many more reliable lines of those species than for any other element. We measured equivalent widths of Fe I and Ti I lines in the spectra using the SPLOT routine of IRAF. We used lines in the cleanest spectral regions available, where the effects of molecular bands and telluric lines were minimized. Because the molecular line strengths depend on stellar temperature and metallicity, we were more successful in finding clean lines for some stars than in others. We accepted partly blended lines for analysis if the blending occurred far enough from the line centre that we were able to use the deblending feature of SPLOT to remove the effect the adjacent line(s).

We did not measure equivalent widths in the spectra of four of the stars we observed for this project. The spectrum of Barnard's Star (LHS 57) had few regions free of molecular bands so that very few unblended atomic lines could

Table 2. Fe and Ti line data

wavelength (Å)	χ (eV)	$\log gf$	EW (mÅ)	$\log N$
HD 33793				
Fe I				
8047.62	0.86	-4.656	91.0	6.42
8075.15	0.91	-5.062	43.0	6.36
8327.06	2.20	-1.525	338.0	6.53
8387.77	2.18	-1.493	355.0	6.52
8514.07	2.20	-2.229	160.0	6.47
8515.11	3.02	-2.073	44.0	6.52
8582.26	2.99	-2.133	38.0	6.44
8611.80	2.85	-1.926	81.0	6.51
8621.60	2.95	-2.321	30.5	6.45
8674.75	2.83	-1.800	95.0	6.48

The full table is available in the electronic version.

be found. LHS 537 and LHS 1718 appear to be double-lined spectroscopic binaries, the analysis of which is beyond the scope of this project. G 30-2 has the broad lines of a fast rotating star, which meant that we were unable to find any unblended lines in its spectrum.

The line data were compiled using the Vienna Atomic Line Database (VALD) (Kupka et al. 1999) and the Kurucz atomic spectral line database (Kurucz & Bell 1995). The line data and equivalent widths measured for each star are listed in Table 2. The original sources of the atomic data for the lines are included in Table 1 of Woolf & Wallerstein (2004).

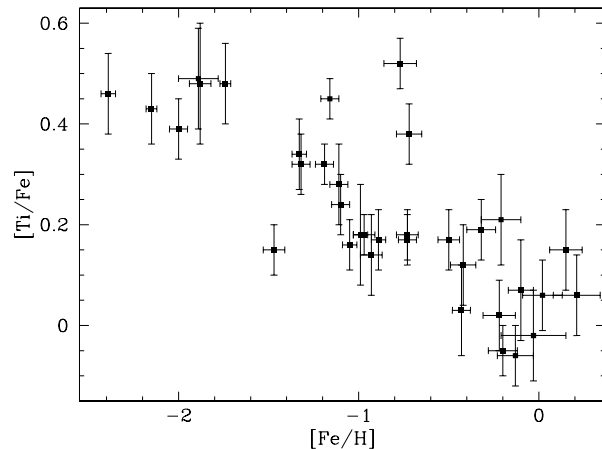
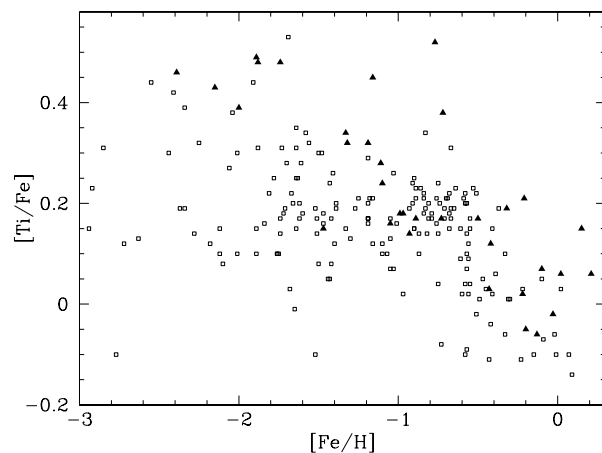
We used MOOG to calculate the abundances from equivalent widths. As discussed previously, determining the stellar chemical abundances is an iterative procedure for these low mass dwarfs which continued until the metallicity calculated using the Fe and Ti abundances equalled the model atmosphere metallicity.

The Fe and Ti abundances we found and the stellar parameters, including α -element weighted metallicity used in the model atmospheres, are listed in Table 3. The uncertainties listed include the effects of the uncertainties of the parallax and photometry data used to derive stellar parameters and the statistical scatter of abundances calculated from different lines in the same star. The ratio $[\text{Ti}/\text{Fe}]$ is plotted against $[\text{Fe}/\text{H}]$ in Figure 1.

We measured equivalent widths of our Fe I and Ti I lines in the solar spectrum (Kurucz, Furenlid, & Brault 1984) where they were not obscured by blending. When we calculated the abundances using the solar equivalent widths and a Kurucz model atmosphere with the solar values $T_{\text{eff}} = 5777$ K, $\log g = 4.44$, and $\xi = 1.15$ km s⁻¹, we found $A(\text{Fe}) = 7.48$ and $A(\text{Ti}) = 4.99$. Altering the gf values of the lines to produce solar gf values would result in very little change in our results, as we have assumed the solar abundances are $A(\text{Fe}) = 7.45$ and $A(\text{Ti}) = 5.02$ (Lodders 2003).

4 DISCUSSION

We have calculated the Fe and Ti abundances of 35 M and K dwarf stars using atomic line equivalent widths measured using spectra with high spectral resolution and high signal-

**Figure 1.** $[\text{Ti}/\text{Fe}]$ vs $[\text{Fe}/\text{H}]$ for 35 M and K dwarf stars.**Figure 2.** $[\text{Ti}/\text{Fe}]$ vs $[\text{Fe}/\text{H}]$. Triangles represent our M and K dwarf stars. Small squares represent the warmer dwarfs and subgiants catalogued by Fulbright (2000).

to-noise ratios. We believe this more than triples the number of dwarf stars in the temperature range of our sample for which chemical abundances have been measured using atomic lines. Our abundance estimates should be more reliable than those of previous studies because we have used updated model atmospheres which include molecular opacity data which is more complete than what was available in any previous models.

The stars we studied have temperatures between 3300 and 4700 K, with a median temperature of 3950 K. They have $[\text{Fe}/\text{H}]$ abundances between -2.4 and $+0.2$. The abundance ratio $[\text{Ti}/\text{Fe}]$ decreases with increasing $[\text{Fe}/\text{H}]$, showing a trend similar to what has been observed for Ti and other α -elements in warmer stars (Wallerstein 1962).

The previous studies using atomic lines and high resolution spectra to measure abundances in dwarf stars in the temperature range of our stars are sparse and included few stars. Mould (1976) studied Kapteyn's Star. He reported $[\text{Fe}/\text{H}] = -0.5 \pm 0.3$, which is 0.5 dex larger than our result. Savanov (1994) studied six M and K dwarfs using two Fe I lines. One star, HD 95735 (Gl 411), was also included in our

Table 3. M and K dwarf parameters and abundances

Star	T_{eff}	\pm	$\log g^a$	\pm	ξ	[M/H]	[Fe/H]	\pm	[Ti/H]	\pm	[Ti/Fe] ^b	\pm
	K				km s ⁻¹							
HD 33793	3570	160	4.96	0.13	2.00	-0.86	-0.99	0.04	-0.81	0.09	0.18	0.10
HD 36395	3760	140	4.71	0.20	1.00	0.15	0.21	0.13	0.27	0.13	0.06	0.08
HD 88230	3970	220	4.51	0.22	1.00	-0.05	-0.03	0.18	-0.05	0.13	-0.02	0.09
HD 95735	3510	150	4.82	0.24	1.00	-0.40	-0.42	0.07	-0.30	0.09	0.12	0.08
HD 97191B	3610	40	4.65	0.05	1.50	-0.01	0.02	0.11	0.08	0.11	0.06	0.07
HD 119850	3650	40	4.79	0.05	0.50	-0.12	-0.10	0.07	-0.03	0.08	0.07	0.10
HD 178126	4530	30	4.57	0.05	1.00	-0.61	-0.72	0.07	-0.34	0.09	0.38	0.06
HD 199305	3720	50	4.67	0.05	2.00	-0.14	-0.13	0.10	-0.19	0.11	-0.06	0.06
HD 217987	3680	130	4.88	0.16	1.00	-0.22	-0.22	0.09	-0.20	0.08	0.02	0.07
LHS 12	3830	40	4.95	0.14	0.50	-0.77	-0.89	0.04	-0.72	0.05	0.17	0.06
LHS 38	3600	30	4.90	0.04	1.00	-0.40	-0.43	0.05	-0.40	0.09	0.03	0.09
LHS 42	3860	30	5.05	0.09	0.50	-0.90	-1.05	0.04	-0.89	0.04	0.16	0.05
LHS 104	3970	30	5.07	0.17	1.00	-1.09	-1.33	0.04	-0.99	0.07	0.34	0.07
LHS 170	4230	30	4.64	0.10	1.00	-0.81	-0.97	0.06	-0.79	0.05	0.18	0.04
LHS 173	4000	20	4.75	0.08	1.00	-0.98	-1.19	0.05	-0.87	0.05	0.32	0.04
LHS 174	3790	20	4.78	0.31	1.00	-0.95	-1.11	0.05	-0.83	0.07	0.28	0.08
LHS 182	3870	30	5.09	0.14	1.00	-1.88	-2.15	0.03	-1.72	0.08	0.43	0.07
LHS 236	4040	20	4.92	0.16	1.50	-1.07	-1.32	0.05	-1.00	0.06	0.32	0.06
LHS 343	4110	30	5.10	0.21	1.00	-1.45	-1.74	0.03	-1.26	0.07	0.48	0.08
LHS 364	3720	30	5.44	0.12	0.50	-0.82	-0.93	0.06	-0.79	0.07	0.14	0.08
LHS 450	3340	20	4.82	0.03	1.00	0.10	0.15	0.09	0.30	0.11	0.15	0.08
LHS 467	3930	40	4.83	0.15	1.25	-0.93	-1.10	0.05	-0.86	0.07	0.24	0.06
LHS 1138	4620	30	4.86	0.45	1.00	-2.17	-2.39	0.04	-1.93	0.08	0.46	0.08
LHS 1482	4100	40	5.0	0.5	2.00	-1.59	-1.88	0.06	-1.40	0.09	0.48	0.12
LHS 1819	4670	40	4.54	0.17	1.50	-0.65	-0.77	0.09	-0.25	0.10	0.52	0.05
LHS 1841	4440	40	5.13	0.20	1.50	-1.18	-1.47	0.06	-1.32	0.07	0.15	0.05
LHS 2161	4500	30	5.0	0.5	1.00	-0.29	-0.32	0.08	-0.13	0.09	0.19	0.06
LHS 2463	4540	30	5.0	0.5	1.50	-1.62	-1.89	0.11	-1.40	0.09	0.49	0.10
LHS 2715	4590	40	4.85	0.11	1.00	-0.95	-1.16	0.05	-0.71	0.06	0.45	0.04
LHS 2938	4490	50	4.44	0.13	1.50	-0.20	-0.21	0.11	0.00	0.16	0.21	0.09
LHS 3084	3780	30	4.88	0.16	1.00	-0.64	-0.73	0.05	-0.56	0.05	0.17	0.05
LHS 3356	3630	30	4.79	0.04	1.50	-0.20	-0.20	0.08	-0.25	0.09	-0.05	0.05
LHS 5337	3780	40	4.59	0.12	0.50	-0.45	-0.50	0.06	-0.33	0.05	0.17	0.06
G 39-36	4400	50	5.0	0.5	1.50	-1.71	-2.00	0.05	-1.61	0.07	0.39	0.06
HIP 27928	4370	30	4.64	0.10	1.00	-0.62	-0.73	0.06	-0.55	0.08	0.18	0.05

^a we used $\log g = 5.0 \pm 0.5$ for the four stars where parallax was unavailable.

^b we use $A(\text{Fe})_{\odot} = 7.45$, $A(\text{Ti})_{\odot} = 5.02$

study. The Fe abundance we derived for the star is 0.42 or 0.57 dex smaller, depending on which gravity Savanov used.

Several researchers have estimated metallicities of low mass dwarfs by fitting synthetic spectra to low resolution observed spectra, $400 < \lambda/\Delta\lambda < 6000$, which included atomic and molecular lines (Jones et al. 1995, 1996; Viti et al. 1997; Leggett et al. 2002). The spectra were for the most part in the near infrared. The metallicities derived were not determined as precisely as is possible using higher resolution spectra, but the method shows what analysis is possible for fainter stars where low resolution spectra are all that is available.

The trend we see in [Ti/Fe] vs [Fe/H] is similar to that seen for warmer stars in the Galaxy. Figure 2 compares our data to the abundances found by Fulbright (2000), who observed field halo and disk stars, most of which are dwarf stars between 5000 and 6500 K. We have made the correction necessary to account for the different assumed solar abundances. Our abundance values do not appear out of place

among the larger set, although our average [Ti/Fe] is higher by about 0.1 dex at most [Fe/H] values. We see a similar relation between our data and that compiled by Gratton et al. (2003). The similar [Ti/Fe] trend was expected since stars of all masses are presumably made from clouds with the same compositions.

Because we selected stars for observation to cover a wide range of metallicity, rather than to statistically represent the low mass dwarfs in a given volume, our results say nothing about the relative numbers of stars with different metallicities.

One goal of this work will be to find a combination of photometric and low-resolution spectral indices which can be used to determine the metallicity of these low mass dwarfs, and to calibrate this method using our observationally determined metallicities. Because the molecular band strengths measured by the spectral indices depend on both the chemical composition and the temperature of a star, the method will need to be sensitive to both properties. We plan

to obtain low resolution spectra of the stars in our list for which TiO and CaH indices have not been measured.

By compiling a statistically significant sample of observationally calibrated metallicity estimates for low mass dwarfs it will be possible to determine the metallicity distribution of these stars in the Galaxy. This will provide observational evidence of whether there is a K and M dwarf problem in our Galaxy similar to the G dwarf problem, where low-metallicity stars are more scarce than predicted by Galactic star formation and chemical evolution models. The answer to this question, positive or negative, will provide important constraints for models of the chemical enrichment of the Galaxy.

ACKNOWLEDGMENTS

We thank David Yong for help getting NextGen models to work in MOOG, Peter Hauschildt for providing pre-release NextGen atmospheres for our use, and Suzanne Hawley for helpful discussions about low mass subdwarfs. This research has made use of the SIMBAD database, operated at CDS, Strasbourg, France. This research has made use of NASA's Astrophysics Data System Bibliographic Services. The authors gratefully acknowledge the financial support of the Kennilworth Fund of the New York Community Trust.

REFERENCES

- Allard, F., Hauschildt, P. H., Schwenke, D., 2000, *ApJ*, 540, 1005
- Audouze, J., Tinsley, B. M., 1976, *ARA&A*, 14, 43
- Cutri, R. M., et al., 2003, *The 2MASS All-Sky Data Release Explanatory Supplement*
- ESA, 1997, *The Hipparcos and Tycho Catalogues* (ESA SP-1200) (Noordwijk: ESA)
- Fulbright, J. P., 2000, *AJ*, 120, 1841
- Gizis, J. E., *AJ*, 113, 806
- Gratton, R. G., Carretta, E., Claudi, R., Lucatello, S., Barbieri, M., 2003, *A&A*, 404, 187
- Harrington, R. S., Dahn, C. C., 1980, *ApJ*, 85, 454
- Hauschildt, P. H., Allard, F., Baron, E., 1999, *ApJ*, 512, 377
- Hawley, S. L., Gizis, J. E., Reid, I. N., *AJ*, 112, 2799
- Jones, H. R. A., Longmore, A. J., Allard, F., Hauschildt, P. H., 1996, *MNRAS*, 280, 77
- Jones, H. R. A., Longmore, A. J., Allard, F., Hauschildt, P. H., Miller, S., Tennyson, J., 1995, *MNRAS*, 277, 767
- Kupka, F., Piskunov, N. E., Ryabchikova, T. A., Stempels, H. C., Weiss, W. W., 1999, *A&AS*, 138, 119
- Kurucz, R. L., Bell, B., 1995, *Kurucz CD-ROM No. 23*, Cambridge, Mass.: Smithsonian Astrophysical Observatory
- Kurucz, R. L., Furenlid, I., Brault, J., 1984, *Solar Flux atlas From 296 to 1300 nm*, National Solar Observatory, Sunspot, NM
- Lee, S.-G., 1984, *AJ*, 89, 702
- Leggett, S. K., Hauschildt, P. H., Allard, F., Geballe, T. R., Baron, E., 2002, *MNRAS*, 332, 78
- Lodders, K., 2003, *ApJ*, 591, 1220
- Luyten, W. J., 1979, *LHS Catalogue*, 2nd edn. Univ. Minnesota Press, Minneapolis
- Mermilliod, J. -C., Mermilliod, M., Hauck, B., 1997, *A&AS*, 124, 349
- Mould, J. R., 1976, *ApJ*, 210, 402
- Ramírez, I., Meléndez, J., 2004, *ApJ*, 609, 417
- Reid, I. N., Hawley, S. L., Gizis, J. E., *AJ*, 110, 1838
- Savanov, I. S., 1994, *Ast. Letters*, 20, 449
- Ségransan, D., Delfosse, X., Forveille, T., Beuzit, L. L., Perrier, C., Udry, S., Mayor, M., 2003a, in *IAU Symp.* 211, *Brown Dwarfs*, 413
- Ségransan, D., Kervella, P., Forveille, T., Queloz, D., 2003b, *A&A*, 397, L5
- Snedden, C. A., 1973, Ph.D. thesis, Univ. of Texas
- van Altena, W. F., Lee, J. T., Hoffleit, E. D., 1995, *The General Catalogue of Trigonometric Stellar Parallaxes*, 4th edn. L. Davis Press, Schenectady, NY
- van den Bergh, S., 1962, *AJ*, 67, 486
- Viti, S., Jones, H. R. A., Schweitzer, A., Allard, F., Hauschildt, P. H., Tennyson, J., Miller, S., Longmore, A. J., 1997, *MNRAS*, 291, 780
- Wallerstein, G., 1962, *ApJS* 6, 407
- Woolf V. M., Wallerstein G., 2004, *MNRAS*, 350, 575